Supplemental Material

Table S1 Sources of non-BB aerosol in the models

MODEL	Anthropogenic emissions	Dust	Volcanic	Sea salt	Default model emission injection height
CAM5	SO_2, BC, and OC from fossil fuel and biofuel combustion: Aerocom2-ACCMIP (Lamarque et al., 2010)	Calculated using friction velocity, soil erodibility, soil moisture.	Non-eruptive volcanic SO2 emissions from AeroCOM (Dentener et al., 2006)	Calculated using 10-m wind speed, sea surface temperature.	Anthrop. emissions: model surface layer. Energy and industry: 100-300 m above surface. BB: evenly distributed from 0 to 1 km.
ECMWF-IFS (CY45R1)	SO_2 , OC and BC from non BB source, from MACCity BB BC and OC: GFAS (Kaiser et al., 2012)	Calculated using surface topography, surface bareness, 10 m wind speed, and ground wetness (Ginoux et al., 2001). Updated with the use of wind gusts.	none	Calculated using 10-m wind speed (Monahan & O'Muircheartaigh, 1986; Morcrette et al., 2009)	BB: Daily injection heights computed by a Plume Rise Model (Paugam et al., 2015).
ECHAM6-SALSA (6.1)	SO_2, BC, and OC from fossil fuel and biofuel combustion: Aerocom2-ACCMIP (Lamarque et al., 2010)	Dust flux calculated on-line using10 m wind speeds, soil clay content and soil moisture from ECHAM6 (Bergman et al., 2012; Tegen et al., 2002)	Emissions from volcanic sources are based on GEIA inventory (Andres & Kasgnoc, 1998)	Calculated using 10-m wind speed (Bergman et al., 2012)	Anthrop. emissions: model surface layer. Energy and industry: 100-300 m above surface. BB: prescribed ecosystem-specific emission profiles from 0 to 6 km. Volcanic: estimated from magnitude of eruption.
GEOS	SO2, NH3, BC, and OC from fossil fuel and biofuel combustion: HTAP2 dataset	5-bins calculated as a function of surface topography, surface bareness, 10 m wind	Global volcanic SO_2 emission inventory by Carn et al. (2017)	5-bins calculated based on met fields	BB emission: evenly distributed within the boundary layer. The rest (du, ss, anthropogenic: oc, bc, su) are injected in the lowest model layer.

		speed, and ground wetness (Ginoux et al., 2001)			Volcanic SO_2 is distributed evenly within a layer defined in Carn's dataset (2017).
GEOS-CHEM (v9-02)	CO, NOx, and SO_2 from EDGAR v3.2-FT2000 (Olivier et al., 2005) NMVOCs: RETRO monthly global inventory for 2000 implemented after (Hu et al., 2015); (Xiao et al., 2008); (Yevich & Logan, 2003); Global anthrop. BC/OC: (Bond et al., 2007) GEIA ammonia emissions (Bouwman et al., 1997) the US NEI05, Canada (CAC), Mexico (BRAVO), Europe (EMEP), East Asian emissions from (Streets et al., 2006) and (Q. Zhang et al., 2009) **Aircraft emissions** BC/OC, sulfur emissions calculated from fuel parameters (Stettler et al., 2011)	Fairlie et al. (2007)	Eruptive and non-eruptive volcanic SO_2 emissions for individual years are from the AEROCOM, (Fisher et al., 2011)	Jaegle et al. (2011)	Species are emitted in the lowest model level, and mixed homogeneously up to the mixing height recalculated in the model.
GISS ModelE OMA	Emissions are taken from Lamarque et al. (2010)	Prognositc (friction velocity, soil erodibility, soil moisture)	Stratospheric AOD prescribed, continous SO_2 AeroCom	Prognostic (10-m wind speed, sea surface temperature)	Anthropogenic emissions from agricuture, domestic, transportation, waster, and shipping sectors are distributed to the model surface layer while those from energy and industry

					sectors are emitted at 100-300 m above surface ; fire emissions are evenly distributed in the boundary layer.
GISS ModelE MATRIX	Emissions are taken from Lamarque et al. (2010)	Prognositc (friction velocity, soil erodibility, soil moisture)	Stratospheric AOD prescribed, continous SO_2 AeroCom	Prognostic (10-m wind speed, sea surface temperature)	Anthropogenic emissions from agricuture, domestic, transportation, waster, and shipping sectors are distributed to the model surface layer while those from energy and industry sectors are emitted at 100-300 m above surface ; fire emissions are evenly distributed in the boundary layer.
GOCART (5 rev. 32)	SO_2, BC, and OC from fossil fuel and biofuel combustion: A2-ACCMIP dataset (Diehl et al., 2012)	Calculated using surface topography, surface bareness, 10-m wind speed, and ground wetness (Ginoux et al., 2001) Update including NDVI (Kim et al., 2013)	Volcanic SO_2 from (A2-MAP), + continuous volcanoes (Diehl et al., 2012)	Calculated based on met fields (Reference?)	BB: evenly distributed within the BL. Volcanic: estimated from magnitude of eruption and volcanic SO_2 index. The rest: injected in the lowest model layer.
OsloCTM2	ECLIPSE V5 emissions for year 2010 (Stohl et al., 2015)	Interactive, (Grini et al., 2005)	Volcanic emissions from AEROCOM (Frank Dentener et al., 2006)	Interactive, (Grini et al., 2005)	Anthropogenic: distributed in the four lowest model layers dependent on emission sectors.
SPRINTARS	SO_2, BC, and OC from fossil fuel and biofuel combustion: HTAP2.	See Appendix A in (T. Takemura et al., 2009)	(Andres & Kasgnoc, 1998)	See Appendix B in (T. Takemura et al., 2009)	BB emission are evenly distributed within the sigma level larger than 0.74. The rest: lowest model layer.

Table S2 Aerosol properties in the models

Model	Aerosol species considered in the model	Aerosol mixing state	Size distributions (size bins if int. mixed)	Aerosol mass extinction efficiency at 550 nm	Aerosol refractive index at 550 nm	Hygroscopicity assumptions for BB-related species	BB-related aerosol aging assumptions	OM/OC conversion factor
CAM5	du, ss, BC, primary organic matter (POM), secondary organic aerosol (SOA and precursor gases), sulfate (and its gaseous precursors SO_2 and DMS)	Internal in the same mode, external between different modes; carbonaceous aerosols are all in the accumulation mode for the three-mode standard representation.	Log-normal size distributions for 3 aerosol modes with the prescribed standard deviation and dry diameter size range for each mode can be found in Table 1 of (Liu et al., 2012)	Wet RI in each mode is calculated based on the volume-weighted means of individual aerosol species. The wet surface mode radius of particles in the mode is calculated based on the Köhler theory. These two parameters are used to parameterize the optical properties of particles in the mode based on (Ghan & Zaveri, 2007).	(1.95,0.79i) for BC; OPAC (Hess et al., 1998) for other species.	0 for BC and 0.1 for POM; SO4=0.507	No aging assumptions applied; upon emission BC and POM are internally mixed with more hygroscopic species in the same accumulation mode, and thus subject to wet scavenging.	1.4
ECMWF-IFS (CY45R1)	du, ss, sulfate, OM, BC	External	See Remy et al. (2019)	See Bozzo et al. (2020)	See Bozzo et al. (2020)	Considered only for optical properties (Remy et al. 2019)	original 80% of BC and 50% of OC are hydrophyllic with e-folding time of 1.16 days	1.5 (for this study)
ECHAM6-	du, ss, OC, BC, sulfate (and its	External	See Figure 1 in	Look-up-tables	Volume weighted	Hygroscopicity: ZSR	no ageing	1.4

SALSA (6.1)	gaseous precursors SO_2 and DMS)		Kokkola et al. (2018)	based on mie calculations for the extinction cross section, asymmetry factor, and single scattering albedo as a function of size parameter and refractive index.	means of individual aerosol species (refractive indices are given by Bergman et al. (2012), Table 5.	method (Jacobson, 2005). BC completely insoluble, 15% of OC is soluble taking as an ideal solute, SO4 hygroscopicity is according to Jacobson (2005).		
GEOS5	du, ss, OC, BC, sulfate, nitrate, and ammonium	External	See table 2 from Chin et al. (2009) except a new sea salt bin (0.03-0.1 um in radius). Nitrate has 3-bins, mean radius 0.27, 2.1, 7.6 um.	See Fig. 2 in Chin et al, 2002	Table 2 from Chin et al. (2009)	Hygroscopic growth factors - see table 3 from Chin et al. (2002)	80% of BC and 50% of OC are hydrophyl. with e-folding time of 2.5 days	1.4
GEOS-CHEM (v9-02)	du, ss, OC, BC, sulfate, nitrates, ammonium, MSA	External	Bulk mass aerosol model, except dust and sea salt. Dust: 4 bins, radius 0.1-1; 1-2; 2-3; 3-6 um. .Sea Salt: fine (0.01-0.5 um, radius) and coarse (0.5-8.0 um, radius).	From GADS/OPAC. Data in m^2/g: sulfate, ammonium and nitrate 2.2; BC 8.0; OC 2.8; SS fine 2.4; SS coarse 0.9; dust from 3.1 to 0.16 from finer to coarser bin	From GADS/OPAC. Sulfate-ammonium-nitrate: 1.43 + 10^-8 i; BC 1.75+0.45 i; OC 1.53+0.006 i; SS 1.5 + 10^-8 i; dust 1.56 + 0.0014 i	Hygroscopicity factors are assigned in 7 RH bin for each species, and Mie scattering and absorption efficiencies recalculated at those bins, and the interpolated at ambient RH online.	Primary hydrophobic fraction of carbonaceous aerosol is converted to hydrofilic with an e-folding time of 1.2 days	2.1 (Turpin & Lim, 2001)
GISS ModelE OMA	du, su coated dust, nitrate coated dust, ss, BC, POM, SOA and precuror gases, sulfate (and its gaseous precursors	Externally mixed, except for sulfate	Effective radii [in um] of bulk aerosol species: SO4 (0.3),		Sulfate (1.528-1.e-7i), nitrate (1.528-1.e-7i), OC (1.527-	80% solubility assumed	No aging	1.4

	SO2 and DMS), ammonium, nitrate, MSA	coated dust	BC (0.1), OC (0.3), NO3 (0.3), seasalt(0.44, 5.), dust (0.46, 1.47, 2.94, 5.88,11.77)		0.014i), BC (1.85-0.71i), sea salt (1.45-0.i), dust (1.564-0.002i)			
GISS ModelE MATRIX	16 mixing state classes (for definition see Bauer et al 2008) containing: sulfate,nitrate,ammium,organics,BC, sea salt, mineral dust and aerosol water.	Prognostic mixing state	Dynamic, Size distributions evolve with microphysical processes		Sulfate (1.528-1.e-7i), nitrate (1.528-1.e-7i), OC (1.527-0.014i), BC (1.85-0.71i), sea salt (1.45-0.i), dust (1.564-0.002i) and water (1.334-3.91e-8i)See Bauer et al 2010	Prognostic, determined by mixing state		1.4
GOCART (5 rev. 32)	du, ss, OC, BC, sulfate (and its gaseous precursors SO_2 and DMS)	External	See table 2 from (Chin et al., 2009)	See Fig. 2 in Chin et al, (2002)	Table 2 from (Chin et al., 2009)	Hygroscopic growth factors - see table 3 below (Chin et al., 2002)	80% of BC and 50% of OC are hydrophyl. with e-folding time of 2 days	1.8
OsloCTM2	du, ss, OC, BC, sulfate, secondary organic aerosols (SOA), nitrate	For fossil fuel and biofuel hydrophilic BC internal mixing, hydropobic BC external mixing. For BB internal mixing of BC and OC.	See Table 2 in (Myhre et al., 2007)	All values in m2/g at 30% RH: Sulfate 3.70, BC fossil fuel external mixture 9.24, OC fossil fuel 4.92, BB(BC + OC) 5.04, nitrate 3.71, sea salt and mineral dust is size dependent	See Table 2 in (Myhre et al., 2007)	Based on (Magi & Hobbs, 2003) (1+1.31*(RH/100)^4.88)	80% of BC and 50% of OC are hydrophillic at the time of emissions. Aging time is dependent on season and latitude (Skeie, Berntsen, Myhre, Tanaka, et al., 2011) part a; (Skeie, Berntsen, Myhre,	1.6 for fossil and biofuel burning; 2.6 for BB

							Pedersen, et al., 2011) part b.	
SPRINTARS (5.5)	du, ss, OC, BC, sulfate (and its gaseous precursors SO_2 and DMS)	external except a half of BC from fuel is internally mixed with OC.	See Table A1 and B1 in Takemura et al. (2009) for dust and sea salt, respectively. The others are assumed to be the log-normal distribution (Toshihiko Takemura et al., 2002)	See (Toshihiko Takemura et al., 2002)	See (Toshihiko Takemura et al., 2002)	See (Toshihiko Takemura et al., 2002)	None	1.6 for fuel; 2.6 for BB

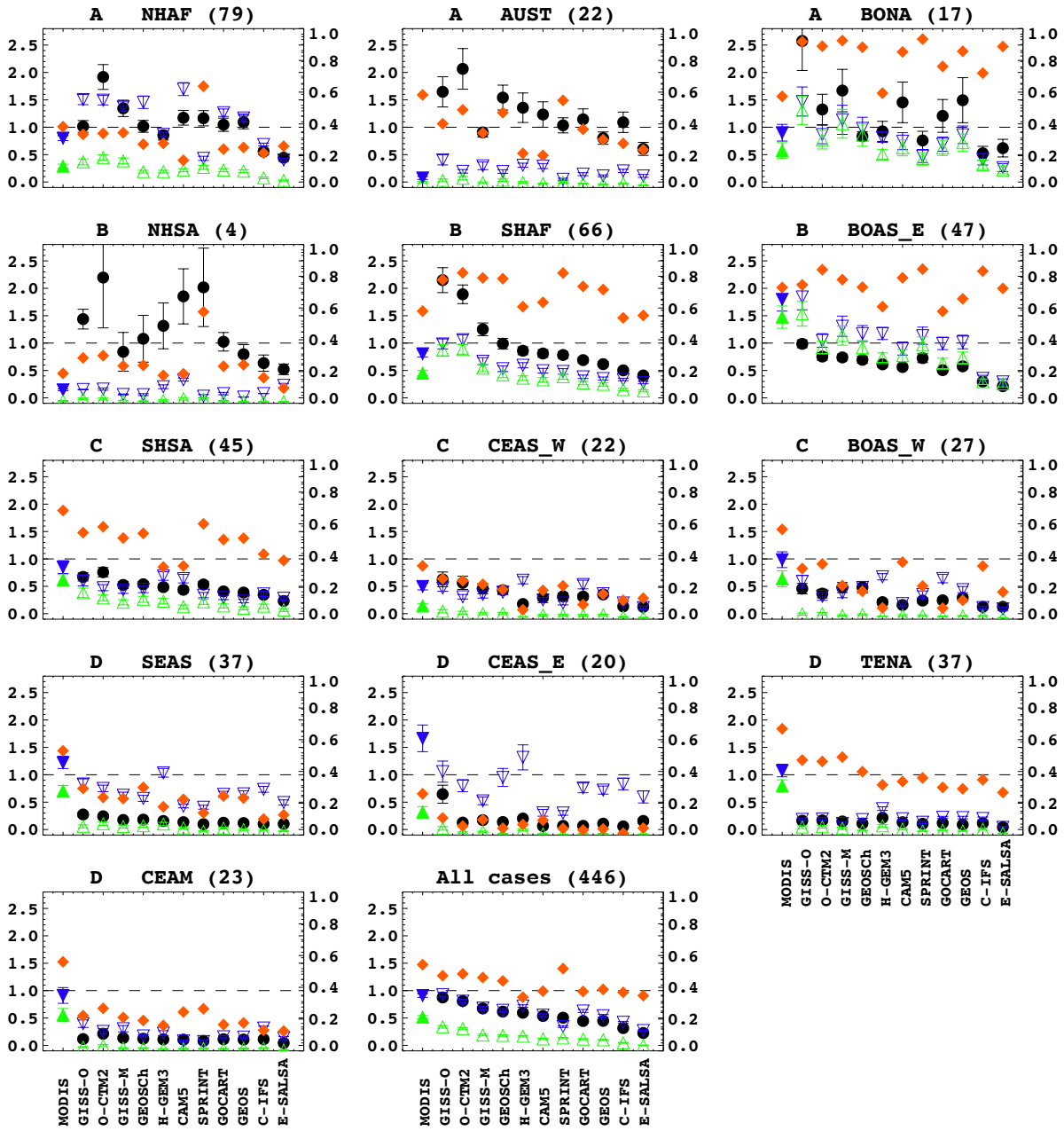

Figure S3 Ratios of model BB AOD to MODIS BB AOD (R_{BB_AOD}) for 11 models, aggregated over each of 13 regions (black dots and left Y axes), plus ratios when aggregated over all regions in the bottom row, right. Shown on the right Y axes are the mean model and MODIS total AOD (blue triangles) and BB AOD (green triangles) for all cases in the region, and the mean BB fraction of total AOD for each model in the region (red diamonds). The group identifiers defined in Section 3.1 are given in the upper left of each panel. Note that the models are ordered in these plots based on the overall R_{BB_AOD}, from highest to lowest, i.e., all individual case averages in a region were used to calculate one arithmetic mean for each model.

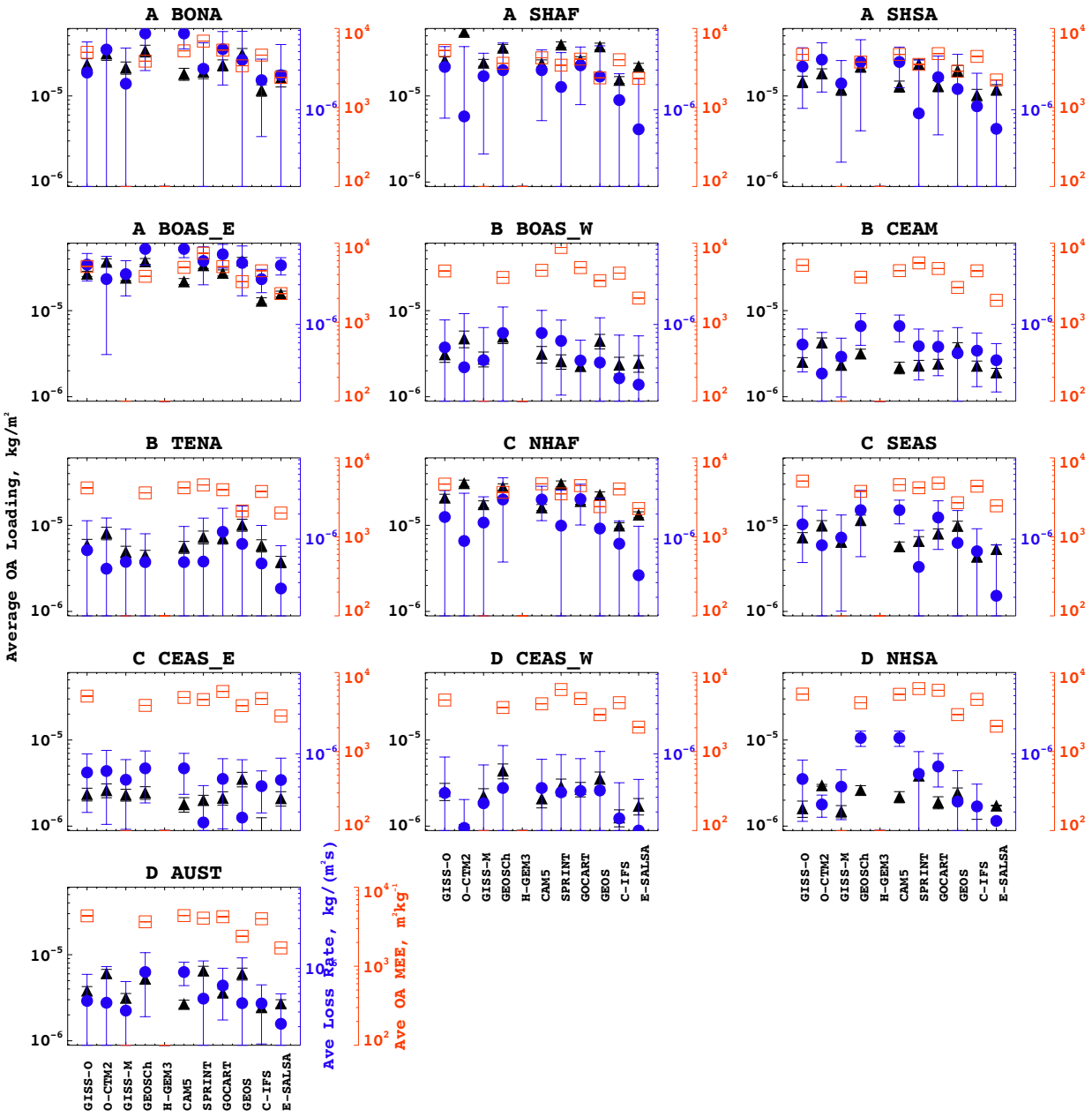

Figure S4 Plots showing the OA Mass Loading (kg/m^2; left Y axis and filled black triangles), OA Loss Frequency (s^{-1}; right blue Y axis and filled blue circles), and OA Mass Extinction Efficiency (m^2/kg; right orange Y axis and open orange squares) for 10 models in each of 13 region-specific panels. Note that Loss Frequency values are missing for the CAM5 model and MEEs are lacking for GISS-M and O-CTM2.

References

Andres, R. J., & Kasgnoc, a. D. (1998). A time-averaged inventory of subaerial volcanic sulfur emissions. *J. Geophys. Res.*, *103*(D19), 25251. https://doi.org/10.1029/98JD02091

Bergman, T., Kerminen, V. M., Korhonen, H., Lehtinen, K. J., Makkonen, R., Arola, A., et al. (2012). Evaluation of the sectional aerosol microphysics module SALSA implementation in ECHAM5-HAM aerosol-climate model. *Geoscientific Model Development*, *5*(3), 845–868. https://doi.org/10.5194/gmd-5-845-2012

Bond, T. C., Bhardwaj, E., Dong, R., Jogani, R., Jung, S., Roden, C., et al. (2007). Historical emissions of black and organic carbon aerosol from energy-related combustion, 1850-2000. *Global Biogeochemical Cycles*, *21*(2). https://doi.org/10.1029/2006GB002840

Bouwman, A. F., Lee, D. S., Asman, W. A. H., Dentener, F. J., Van Der Hoek, K. W., & Olivier, J. G. J. (1997). A global high-resolution emission inventory for ammonia. *Global Biogeochemical Cycles*, *11*(4), 561–587. https://doi.org/10.1029/97GB02266

Bozzo, A., Benedetti, A., Flemming, J., Kipling, Z., and Rémy, S.: An aerosol climatology for global models based on the tropospheric aerosol scheme in the Integrated Forecasting System of ECMWF, Geosci. Model Dev., 13, 1007–1034, https://doi.org/10.5194/gmd-13-1007-2020, 2020.

Carn, S. A., Fioletov, V. E., Mclinden, C. A., Li, C., & Krotkov, N. A. (2017). A decade of global volcanic SO2emissions measured from space. *Scientific Reports*, *7*, 1–12. https://doi.org/10.1038/srep44095

Chin, M., Ginoux, P., Kinne, S., Torres, O., Holben, B. N., Duncan, B. N., et al. (2002). Tropospheric aerosol optical thickness from the GOCART model and comparisons with satellite and sun photometer measurements. *Journal of the Atmospheric Sciences*, *59*, 461–483.

Chin, M., Diehl, T., Dubovik, O., Eck, T. F., Holben, B. N., Sinyuk, A., & Streets, D. G. (2009). Light absorption by pollution, dust, and biomass burning aerosols: a global model study and evaluation with AERONET measurements. *Annales Geophysicae*, *27*(9), 3439–3464. https://doi.org/10.5194/angeo-27-3439-2009

Dentener, F., Kinne, S., Bond, T., Boucher, O., Cofala, J., Generoso, S., et al. (2006). Emissions of primary aerosol and precursor gases in the years 2000 and 1750 prescribed data-sets for AeroCom. *Atmospheric Chemistry and Physics*, *6*, 4321–4344. Retrieved from http://www.atmos-chem-phys.net/6/4321/2006/

Dentener, F., Drevet, J., Lamarque, J. F., Bey, I., Eickhout, B., Fiore, A. M., et al. (2006). Nitrogen and sulfur deposition on regional and global scales: A multimodel evaluation. *Global Biogeochemical Cycles*, *20*(4). https://doi.org/10.1029/2005GB002672

Diehl, T., Heil, A., Chin, M., Pan, X., Streets, D., Schultz, M., & Kinne, S. (2012). Anthropogenic, biomass burning, and volcanic emissions of black carbon, organic carbon, and SO2 from 1980 to 2010 for hindcast model experiments. *Atmospheric Chemistry and Physics Discussion*, *12*, 24895–24954. https://doi.org/10.5194/acpd-12-24895-2012

Duncan Fairlie, T., Jacob, D. J., & Park, R. J. (2007). The impact of transpacific transport of mineral dust in the United States. *Atmospheric Environment*, *41*(6), 1251–1266. https://doi.org/10.1016/j.atmosenv.2006.09.048

Fisher, J. A., Jacob, D. J., Wang, Q., Bahreini, R., Carouge, C. C., Cubison, M. J., et al. (2011). Sources, distribution, and acidity of sulfate-ammonium aerosol in the Arctic in winter-spring. *Atmospheric Environment*, *45*(39), 7301–7318. https://doi.org/10.1016/j.atmosenv.2011.08.030

Ghan, S. J., & Zaveri, R. A. (2007). Parameterization of optical properties for hydrated internally mixed aerosol. *Journal of Geophysical Research Atmospheres*, *112*(10). https://doi.org/10.1029/2006JD007927

Ginoux, P., Chin, M., Tegen, I., Prospero, J. M., Holben, B., Dubovik, O., & Lin, S.-J. (2001). Sources and distributions of dust aerosols simulated with the GOCART model. *Journal of Geophysical Research*, *106*(D17), 20255–20274. https://doi.org/10.1029/2000JD000053

Gong, S. L. (2003). A parameterization of sea-salt aerosol source function for sub- and super-micron particles. *Global Biogeochemical Cycles*, *17*(4), n/a-n/a. https://doi.org/10.1029/2003GB002079

Grini, A., Korhonen, H., Lehtinen, K. E. J., Isaksen, I. S. A., & Kulmala, M. (2005). A combined photochemistry/aerosol dynamics model: model development and a study of new particle formation. *Boreal Env Res*, *10*, 525–541.

Hess, M., Koepke, P., & Schult, I. (1998). Optical Properties of Aerosols and Clouds: The Software Package OPAC. *Bulletin of the American Meteorological Society*, *79*(5), 831–844. https://doi.org/10.1175/1520-0477(1998)079<0831:OPOAAC>2.0.CO;2

Hu, W. W., Campuzano-Jost, P., Palm, B. B., Day, D. A., Ortega, A. M., Hayes, P. L., et al. (2015). Characterization of a real-time tracer for isoprene epoxydiols-derived secondary organic aerosol (IEPOX-SOA) from aerosol mass spectrometer measurements. *Atmospheric Chemistry and Physics*, *15*(20), 11807–11833. https://doi.org/10.5194/acp-15-11807-2015

Jacobson, M. Z. (2005). *Fundamentals of Atmospheric Modeling* (Second edi). New York: Cambridge University Press.

Jaeglé, L., Quinn, P. K., Bates, T. S., Alexander, B., & Lin, J. T. (2011). Global distribution of sea salt aerosols: New constraints from in situ and remote sensing observations. *Atmospheric Chemistry and Physics*, *11*(7), 3137–3157. https://doi.org/10.5194/acp-11-3137-2011

Kaiser, J. W., Heil, A., Andreae, M. O., Benedetti, A., Chubarova, N., Jones, L., et al. (2012). Biomass burning emissions estimated with a global fire assimilation system based on observed fire radiative power. *Biogeosciences*, *9*, 527–554. https://doi.org/doi:10.5194/bg-9-527-2012

Kettle, A. J., & Andreae, M. O. (2000). Flux of dimethylsulfide from the oceans: A comparison of updated data sets and flux models. *Journal of Geophysical Research: Atmospheres*, *105*(D22), 26793–26808. https://doi.org/10.1029/2000JD900252

Kim, D., Chin, M., Bian, H., Tan, Q., Brown, M. E., Zheng, T., et al. (2013). The effect of the dynamic surface bareness on dust source function, emission, and distribution. *Journal of Geophysical Research Atmospheres*, *118*(2), 871–886. https://doi.org/10.1029/2012JD017907

Kokkola, H., Kühn, T., Laakso, A., Bergman, T., Lehtinen, K. E. J., Mielonen, T., et al. (2018). SALSA2.0: The sectional aerosol module of the aerosol-chemistry-climate model ECHAM6.3.0-HAM2.3-MOZ1.0. *Geoscientific Model Development Discussions*, (April), 1–43. https://doi.org/10.5194/gmd-2018-47

Lamarque, J. F., Bond, T. C., Eyring, V., Granier, C., Heil, A., Klimont, Z., et al. (2010). Historical (1850–2000) gridded anthropogenic and biomass burning emissions of reactive gases and aerosols: methodology and application. *Atmos. Chem. Phys.*, *10*(15), 7017–7039. https://doi.org/10.5194/acp-10-7017-2010

Liss, P. S., & Merlivat, L. (1986). Air-sea gas exchange rates: introduction and synthesis. In *The Role of Air-Sea Exchange in Geochemical Cycling* (pp. 113–127). https://doi.org/10.1007/978-94-009-4738-2_5

Liu, X., Easter, R. C., Ghan, S. J., Zaveri, R., Rasch, P., Shi, X., Lamarque, J.-F., Gettelman, A., Morrison, H., Vitt, F., Conley, A., Park, S., Neale, R., Hannay, C., Ekman, A. M. L., Hess, P., Mahowald, N., Collins, W., Iacono, M. J., Bretherton, C. S., Flanner, M. G., and Mitchell, D.: Toward a minimal representation of aerosols in climate models: description and evaluation in the Community Atmosphere Model CAM5, Geosci. Model Dev., 5, 709-739, doi:10.5194/gmd-5-709-2012, 2012.

Magi, B. I., & Hobbs, P. V. (2003). Effects of humidity on aerosols in southern Africa during the biomass burning season. *Journal of Geophysical Research: Atmospheres*, *108*(D13), n/a-n/a. https://doi.org/10.1029/2002JD002144

Monahan, E. C., & O'Muircheartaigh, I. G. (1986). Whitecaps and the passive remote sensing of the ocean surface. *International Journal of Remote Sensing*, *7*(5), 627–642. https://doi.org/10.1080/01431168608954716

Morcrette, J.-J., Boucher, O., Jones, L., Salmond, D., Bechtold, P., Beljaars, A., et al. (2009). Aerosol analysis and forecast in the European Centre for Medium-Range Weather Forecasts Integrated Forecast System: Forward modeling. *Journal of Geophysical Research*, *114*(D6), D06206. https://doi.org/10.1029/2008JD011235

Myhre, G., Bellouin, N., Berglen, T. F., Berntsen, T. K., Boucher, O., Grini, A., et al. (2007). Comparison of the radiative properties and direct radiative effect of aerosols from a global aerosol model and remote sensing data over ocean. *Tellus, Series B: Chemical and Physical Meteorology*, *59*(1), 115–129. https://doi.org/10.1111/j.1600-0889.2006.00226.x

Olivier, J. G. J., Van Aardenne, J. A., Dentener, F. J., Pagliari, V., Ganzeveld, L. N., & Peters, J. A. H. W. (2005). Recent trends in global greenhouse gas emissions:regional trends 1970–2000 and spatial distributionof key sources in 2000. *Environmental Sciences*, *2*(2–3), 81–99. https://doi.org/10.1080/15693430500400345

Paugam, R., Wooster, M., Atherton, J., Freitas, S. R., Schultz, M. G., & Kaiser, J. W. (2015). Development and optimization of a wildfire plume rise model based on remote sensing data inputs – Part 2. *Atmospheric Chemistry and Physics Discussions*, *15*(6), 9815–9895. https://doi.org/10.5194/acpd-15-9815-2015

Reddy, M. S., Boucher, O., Bellouin, N., Schulz, M., Balkanski, Y., Dufresne, J. L., & Pham, M. (2005). Estimates of global multicomponent aerosol optical depth and direct radiative perturbation in the Laboratoire de Météorologie Dynamique general circulation model. *Journal of Geophysical Research D: Atmospheres*, *110*(10), 1–16. https://doi.org/10.1029/2004JD004757

Rémy, S., Kipling, Z., Flemming, J., Boucher, O., Nabat, P., Michou, M., Bozzo, A., Ades, M., Huijnen, V., Benedetti, A., Engelen, R., Peuch, V.-H., and Morcrette, J.-J.: Description and evaluation of the tropospheric aerosol scheme in the European Centre for Medium-Range Weather Forecasts (ECMWF) Integrated Forecasting System (IFS-AER, cycle 45R1), Geosci. Model Dev., 12, 4627–4659, https://doi.org/10.5194/gmd-12-4627-2019, 2019.

Skeie, R. B., Berntsen, T. K., Myhre, G., Tanaka, K., Kvaleväg, M. M., & Hoyle, C. R. (2011). Anthropogenic radiative forcing time series from pre-industrial times until 2010. *Atmospheric Chemistry and Physics*, *11*(22), 11827–11857. https://doi.org/10.5194/acp-11-11827-2011

Skeie, R. B., Berntsen, T., Myhre, G., Pedersen, C. A., Strãm, J., Gerland, S., & Ogren, J. A. (2011). Black carbon in the atmosphere and snow, from pre-industrial times until present. *Atmospheric Chemistry and Physics*, *11*(14), 6809–6836. https://doi.org/10.5194/acp-11-6809-2011

Smith, M. H., & Harrison, N. M. (1998). The sea spray generation function. *Journal of Aerosol Science*, *29*, S189–S190. https://doi.org/https://doi.org/10.1016/S0021-8502(98)00280-8

Stettler, M. E. J., Eastham, S., & Barrett, S. R. H. (2011). Air quality and public health impacts of UK airports. Part I: Emissions. *Atmospheric Environment*, *45*(31), 5415–5424. https://doi.org/10.1016/j.atmosenv.2011.07.012

Stohl, A., Aamaas, B., Amann, M., Baker, L. H., Bellouin, N., Berntsen, T. K., et al. (2015). Evaluating the climate and air quality impacts of short-lived pollutants. *Atmospheric Chemistry and Physics*, *15*(18), 10529–10566. https://doi.org/10.5194/acp-15-10529-2015

Streets, D. G., Zhang, Q., Wang, L., He, K., Hao, J., Wu, Y., et al. (2006). Revisiting China's CO emissions after the Transport and Chemical Evolution over the Pacific (TRACE-P) mission: Synthesis of inventories, atmospheric modeling, and observations. *Journal of Geophysical Research Atmospheres*, *111*(14). https://doi.org/10.1029/2006JD007118

Takemura, T., Nakajima, T., Dubovik, O., Holben, B. N., & Kinne, S. (2002). Single-scattering albedo and radiative forcing of various aerosol species with a global three-dimensional model. *Journal of Climate*, *15*(4), 333–352. https://doi.org/10.1175/1520-0442(2002)015<0333:SSAARF>2.0.CO;2

Takemura, T., Egashira, M., Matsuzawa, K., Ichijo, H., O'Ishi, R., & Abe-Ouchi, A. (2009). A simulation of the global distribution and radiative forcing of soil dust aerosols at the Last Glacial Maximum. *Atmospheric Chemistry and Physics*, *9*(9), 3061–3073. https://doi.org/10.5194/acp-9-3061-2009

Tegen, I., Harrison, S. P., Kohfeld, K., Prentice, I. C., Coe, M., & Heimann, M. (2002). Impact of vegetation and preferential source areas on global dust aerosol: Results from a model study. *Journal of Geophysical Research Atmospheres*, *107*(21). https://doi.org/10.1029/2001JD000963

Turpin, B. J., & Lim, H. J. (2001). Species contributions to pm2.5 mass concentrations: Revisiting common assumptions for estimating organic mass. *Aerosol Science and Technology*, *35*(1), 602–610. https://doi.org/10.1080/02786820119445

Vignati, E., Wilson, J., & Stier, P. (2004). M7: An efficient size-resolved aerosol microphysics module for large-scale aerosol transport models. *Journal of Geophysical Research D: Atmospheres*, *109*(22), 1–17. https://doi.org/10.1029/2003JD004485

Woodward, S. (2001). Modeling the atmospheric life cycle and radiative impact of mineral dust in the Hadley Centre climate model. *Journal of Geophysical Research: Atmospheres*, *106*(D16), 18155–18166. https://doi.org/10.1029/2000JD900795

Xiao, Y., Logan, J. A., Jacob, D. J., Hudman, R. C., Yantosca, R., & Blake, D. R. (2008). Global budget of ethane and regional constraints on U.S. sources. *Journal of Geophysical Research Atmospheres*, *113*(21). https://doi.org/10.1029/2007JD009415

Yevich, R., & Logan, J. A. (2003). An assessment of biofuel use and burning of agricultural waste in the developing world. *Global Biogeochemical Cycles*, *17*(4), n/a-n/a. https://doi.org/10.1029/2002GB001952

Zhang, K., O'Donnell, D., Kazil, J., Stier, P., Kinne, S., Lohmann, U., et al. (2012). The global aerosol-climate model ECHAM-HAM, version 2: sensitivity to improvements in process representations. *Atmos. Chem. Phys.*, *12*, 8911–8949. Retrieved from https://doi.org/10.5194/acp-12-8911-2012

Zhang, Q., Streets, D. G., Carmichael, G. R., He, K. B., Huo, H., Kannari, A., et al. (2009). Asian emissions in 2006 for the NASA INTEX-B mission. *Atmospheric Chemistry and Physics*, *9*(14), 5131–5153. https://doi.org/10.5194/acp-9-5131-2009